Advances in Geosciences, 6, 29–33, 2006
SRef-ID: 1680-7359/adgeo/2006-6-29
European Geosciences Union

Advances in Geosciences

Coupled model simulations of mid-Holocene ENSO and comparisons with coral oxygen isotope records

J. Brown[1], **M. Collins**[2], **and A. Tudhope**[3]

[1]Centre for Global Atmospheric Modelling, Department of Meteorology, University of Reading, Reading, UK
[2]Hadley Centre for Climate Prediction and Research, Met Office, Exeter, UK
[3]School of Geosciences, University of Edinburgh, Edinburgh, UK

Received: 15 August 2005 – Revised: 18 October 2005 – Accepted: 19 October 2005 – Published: 9 January 2006

Abstract. The sensitivity of El Niño-Southern Oscillation (ENSO) to changes in mean climate is investigated for simulations of pre-industrial and mid-Holocene (6000 years before present) climate using the Hadley Centre coupled atmosphere-ocean model, HadCM3. Orbitally-forced changes in insolation in the mid-Holocene produce changes in seasonality which may alter ENSO amplitude and frequency. The model simulations are compared with mid-Holocene fossil coral oxygen isotope records from the western Pacific Warm Pool. The coral records imply a reduction of around 60% in the amplitude of interannual variability associated with ENSO in the mid-Holocene, while the model simulates a smaller reduction in ENSO amplitude of around 10%. The model also simulates a slight shift to longer period variability and a weakening of ENSO phase-locking to the seasonal cycle in the mid-Holocene. There is little change in the pattern of ENSO tropical precipitation teleconnections in the simulated mid-Holocene climate.

1 Introduction

Palaeoclimate records indicate that El Niño-Southern Oscillation (ENSO) may have been weaker than present or absent in the early and mid-Holocene (∼10 000 to ∼5000 years ago) (Sandweiss et al., 1996; Rodbell et al., 1999; Tudhope et al., 2001). Changes in the timing of perihelion resulted in altered solar forcing at this time, with increased Northern Hemisphere and tropical seasonality, although annual average insolation was virtually unchanged from the present. Previous modelling studies have found changes in ENSO amplitude and frequency in response to Holocene orbital forcing (e.g. Clement et al., 2000, 2001; Otto-Bliesner et al., 2003). We use the HadCM3 coupled atmosphere-ocean model to simulate mid-Holocene and pre-industrial climate. We consider the change in mean climate in the mid-Holocene, and the change in interannual sea surface temperature (SST) variability, ENSO amplitude and frequency. We compare the model results with modern and fossil coral oxygen isotope records from coastal Papua New Guinea in the western Pacific Warm Pool. The ultimate aim of this study is to evaluate the model's ability to simulate past climates in order to build confidence in its ability to simulate future anthropogenic climate change.

Correspondence to: J. Brown
(josephine.brown@reading.ac.uk)

2 Mid-Holocene coral records

Coral oxygen isotope records have been obtained from living and fossil corals from the Huon Peninsula, Madang and Laing Island on the north coast of Papua New Guinea (Fig. 1). The oxygen isotope ratio (δ^{18}O) from living coral at the three sites is found to be strongly correlated with ENSO activity due to cooler (warmer) SSTs and decreased (increased) precipitation during El Niño (La Niña) events (Tudhope et al., 1995, 2001). Selected modern and fossil coral oxygen isotope records from the mid- and late Holocene are shown in Fig. 2. The oxygen isotope ratios in mid-Holocene fossil coral from 6500 years ago (6.5 ka) show weaker variability at ENSO periods, a reduction of 60% relative to 20th century amplitudes, while the amplitude in the late Holocene (2.7 ka) coral record is similar to the modern amplitude (Tudhope et al., 2001).

The coral oxygen isotope ratio reflects changes in both SST and local ocean isotopic ratio, which is influenced by the balance between precipitation and evaporation. While SST and precipitation vary together for modern ENSO events at the coral site (e.g. Tudhope et al., 1995), this relationship may differ for past climates. For example, Gagan et al. (2004) examine coral oxygen isotope ratios and Sr/Ca

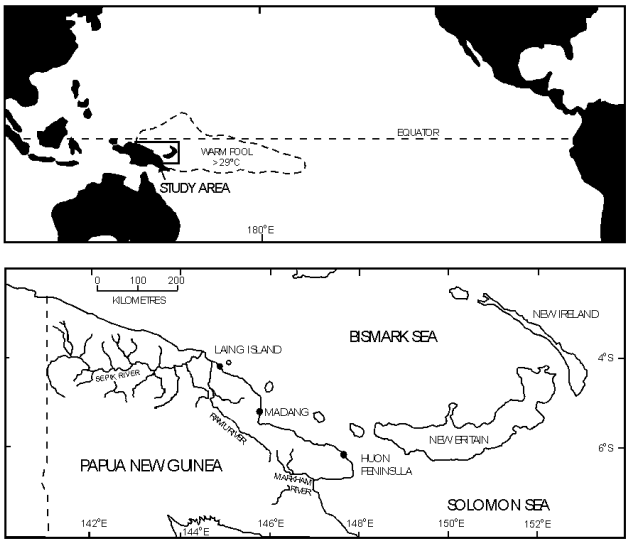

Fig. 1. Location of Laing Island, Madang and Huon Peninsula coral sites (adapted from Tudhope et al. (2001)).

ratios at 6.2 ka from Great Barrier Reef fossil corals and find that SST variability associated with ENSO was reduced by 20% while precipitation variability was reduced by around 70% compared with late 20th century values. It is possible that changes in ENSO precipitation teleconnections may contribute to the large reduction in amplitude in the Huon Peninsula records, as the signal at the Papua New Guinea site is predominantly influenced by precipitation rather than SST for modern coral records (Tudhope et al., 1995). We therefore investigate the changes in modelled ENSO precipitation and SST variability in comparison with the proxy record.

3 Modelled mid-Holocene climate

HadCM3 is a fully coupled atmosphere-ocean model with 3.75° longitude and 2.5° latitude horizontal resolution and 19 levels in the atmospheric component, as described by Pope et al. (2000). The ocean component has a uniform resolution of 1.25° with 20 vertical levels (Gordon et al., 2000). The model exhibits no significant climate drift, and so can perform multi-century integrations without flux correction. HadCM3 has been shown to simulate ENSO as well as other state-of-the-art coupled models, with an amplitude and frequency which is broadly similar to observations. Known biases in the model climate which may influence the evolution of ENSO temperature and precipitation anomalies include a cold bias in the central equatorial Pacific Ocean and a warm bias over the Maritime continent (e.g. Inness et al., 2003; Turner et al., 2005). The equatorial Pacific trade winds are stronger than observed, and convection tends to be confined to the western Pacific Warm Pool and stronger than observed.

The pre-industrial climate simulation is carried out using modern orbital parameters, vegetation coverage and continental ice sheets, and an atmospheric CO_2 concentration of 280 ppmv. The orbital parameters are altered for the mid-Holocene simulation, with all other boundary conditions the same as for the pre-industrial simulation. The model is run for 100 years in each case and flux corrections are not applied. Figure 3 shows the seasonal (DJF and JJA) surface temperature anomalies in the mid-Holocene climate in response to the change in insolation. In the mid-Holocene, Northern Hemisphere mid-latitude continental surface temperatures are increased in summer and decreased in winter. Due to the increased Northern Hemisphere summer land-sea temperature gradient, the Asian summer monsoon precipitation is increased, although interannual variability of monsoon strength is reduced according to both dynamical and precipitation indices (not shown). The Sahel region in Africa also experiences increased precipitation during the summer monsoon, with a slight northward shift in the region of maximum precipitation.

The mean state of the tropical Pacific in the mid-Holocene remains the subject of some debate. Lake sediment records from Ecuador indicate fewer strong El Niño events in the mid-Holocene, which Rodbell et al. (1999) interpret as evidence for warmer eastern Pacific SSTs. More recent studies (e.g. Clement et al., 2000; Liu et al., 2003) have argued that these lake sediment records are consistent with a cooler eastern Pacific. Mg/Ca records from near the Galapagos suggest mid-Holocene cooling in the eastern Pacific, with an enhanced zonal SST gradient and strengthened trade winds (Koutavas et al., 2002). Coral evidence of warming in the western Pacific (Gagan et al., 1998) may have resulted in an increased zonal SST gradient across the Pacific. Mollusk distributions on the coast of Peru imply locally warmer waters, which may be due to changes in coastal SSTs and upwelling or large-scale El Niño-like conditions (Sandweiss et al., 1996). Several previous modelling studies have suggested that the mean tropical ocean state was La Niña-like in the mid-Holocene with a relative cooling in the eastern Pacific, in some cases accompanied by a strengthening of the trade winds and changes in the distribution of precipitation (e.g. Otto-Bliesner, 1999; Bush, 1999; Liu et al., 2003).

The modelled change in tropical SSTs from mid-Holocene to pre-industrial climate is shown in Fig. 3. There is a cooling of up to 1°C in the central and eastern tropical Pacific in DJF, while in JJA SSTs warm slightly on the equator in the eastern Pacific with cooling off the equator and in the central and western equatorial Pacific. The annual average zonal SST gradient in the equatorial Pacific is unchanged in the mid-Holocene simulation, although the zonal SST gradient is seasonally strengthened following boreal winter and weakened following boreal summer. The easterly trade winds also undergo seasonal changes in the mid-Holocene simulation, with a strengthening from boreal summer onwards in the central and western Pacific (not shown), consistent with previous modelling studies.

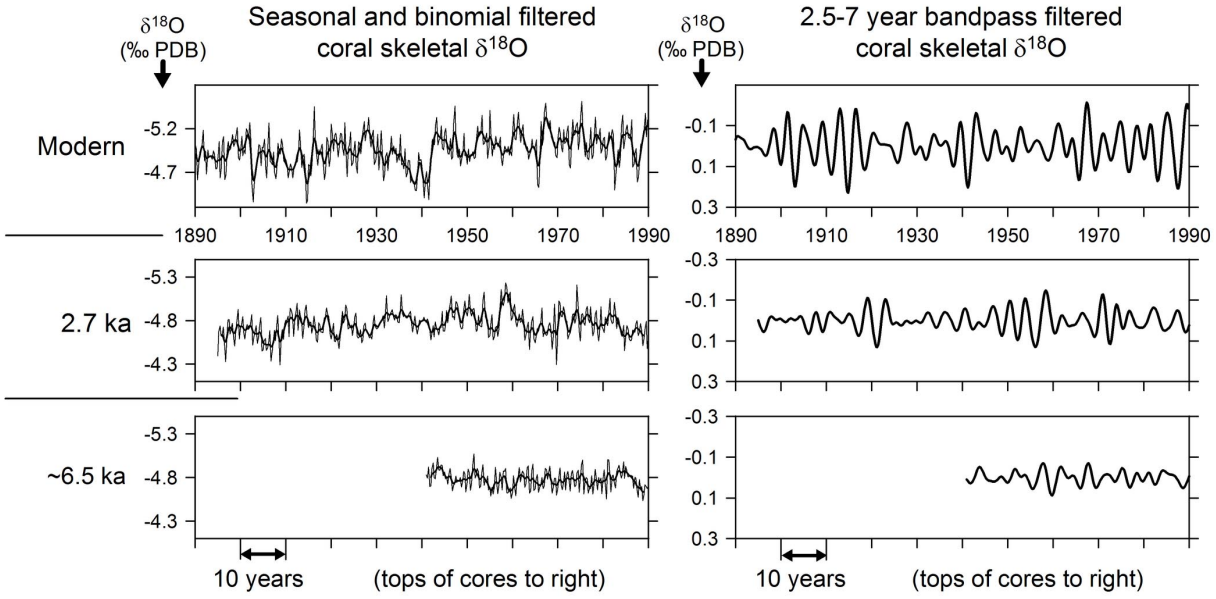

Fig. 2. Oxygen isotope ratios from Papua New Guinea coral. Left: Seasonal resolution (thin lines) and 2.25-year binomial-filtered skeletal δ^{18}O records from fossil corals of 2.7 ka and 6.5 ka age, with the record from a modern coral shown for comparison. Right: 2.5–7 year (ENSO) bandpass-filtered coral δ^{18}O anomalies (adapted from Tudhope et al. (2001)). Coral δ^{18}O values are given in permil (PDB).

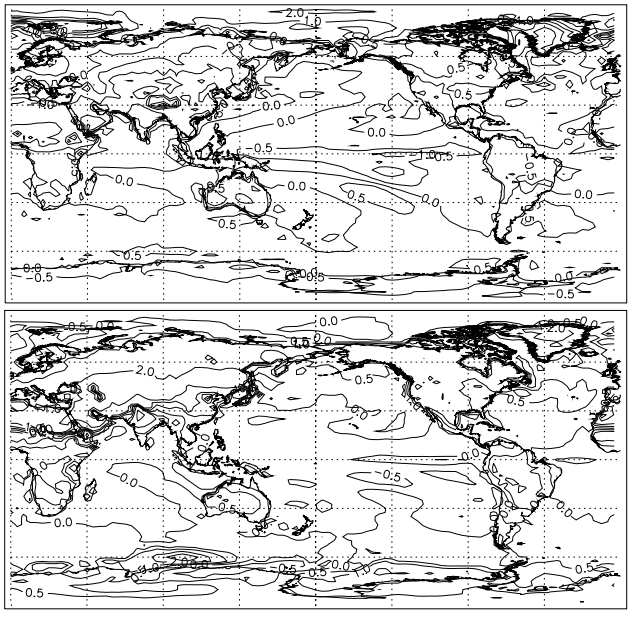

Fig. 3. Difference between model-simulated mid-Holocene and pre-industrial surface temperature for DJF (above) and JJA (below). Contour interval is 0.5°C.

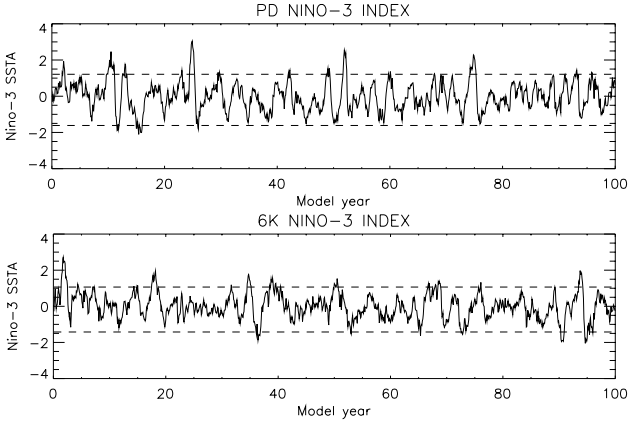

Fig. 4. Niño-3 SST anomalies (°C) for 100-year pre-industrial (above) and mid-Holocene (below) climate simulations. Dashed line indicates ±2 standard deviations of the Niño-3 anomalies. Monthly mean values are shown with the seasonal cycle removed.

4 Modelled mid-Holocene ENSO

The timeseries of the SST anomaly in the Ninõ-3 region (5° N–5° S, 150–90° W) is calculated for the 100-year pre-industrial and mid-Holocene simulations (Fig. 4). The standard deviation of the Niño-3 index is 0.81°C for the pre-industrial run and 0.71°C for the mid-Holocene run, representing a reduction in ENSO amplitude of 12%. The difference between the amplitude of ENSO in the two runs is within the range of internal model interdecadal variability in a 1000-year HadCM3 control run (Collins, 2000a), therefore it is difficult to make statistically robust conclusions.

The power spectrum of Niño-3 SST anomalies for HadISST observed SSTs from 1949–2002 (Rayner et al., 2003) is compared with the pre-industrial and mid-Holocene Niño-3 spectra in Fig. 5. The modelled pre-industrial ENSO has maximum power at periods of 2–3 and 5 years, while the mid-Holocene ENSO has maximum power at slightly longer

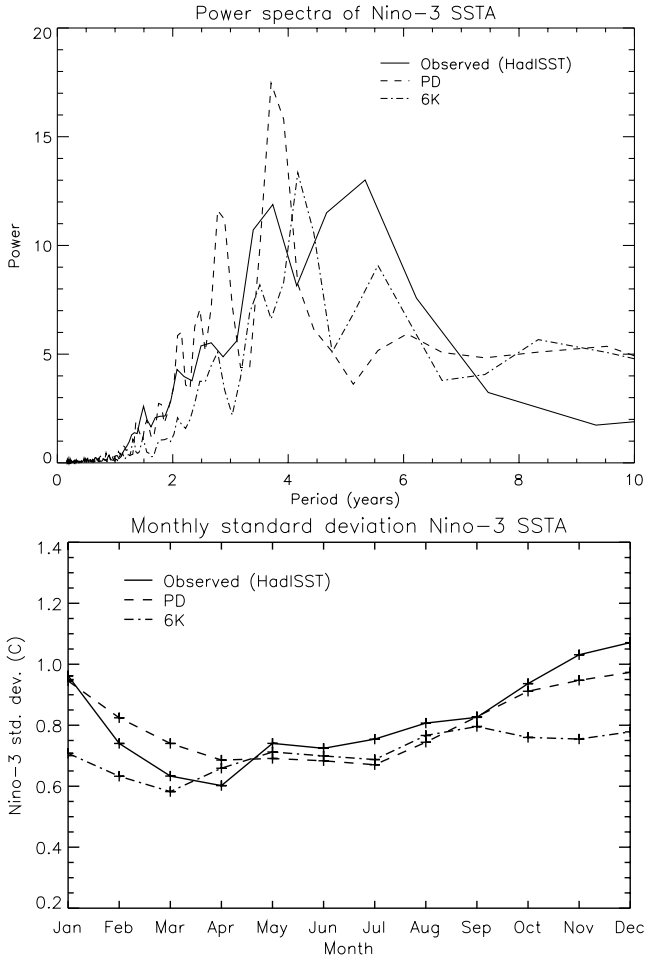

Fig. 5. Spectra of HadISST observed (solid line), pre-industrial (dashed line) and mid-Holocene (dot-dashed line) Niño-3 SST anomalies (above); seasonal cycle of HadISST observed (solid line), pre-industrial (dashed line) and mid-Holocene (dot-dashed line) standard deviation of Niño-3 SST anomalies (below).

periods of 4.5 and 5.5 years. The mean annual cycle of Niño-3 SST anomalies is also shown in Fig. 5 in comparison with HadISST observations. The modelled pre-industrial ENSO shows phase-locking to the annual cycle in broad agreement with observations, with maximum amplitude in December although the minimum is later than the observed April minimum. The simulated mid-Holocene ENSO has a weaker phase-locking to the seasonal cycle, with a strong reduction in amplitude in the period September–April.

The precipitation response to ENSO is investigated using the correlation between monthly anomalies of Niño-3 SST and precipitation, as shown in Fig. 6. In the pre-industrial case, the model simulates a positive Niño3 SST-precipitation correlation over the western Pacific Warm Pool region corresponding to the coral sites, whereas in observations this relationship is reversed with reduced precipitation during warm El Niño events (e.g. Dai and Wigley, 2000). This is a known bias in HadCM3, with the overly strong trades confining the

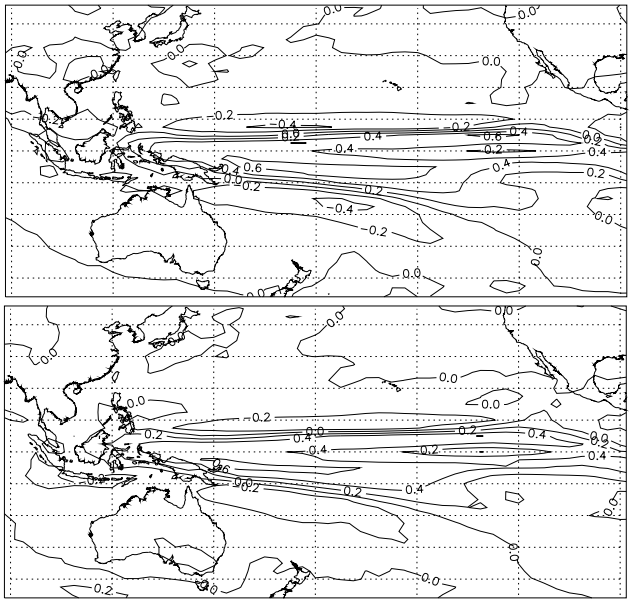

Fig. 6. Correlation between monthly Niño-3 SST anomalies and precipitation anomalies in pre-industrial (above) and mid-Holocene (below) climate simulations, highlighting ENSO teleconnection patterns. Contour interval is 0.2.

eastward expansion of the Warm Pool and associated convection during El Niño events (e.g. Inness et al., 2003; Turner et al., 2005). In the mid-Holocene, the model simulates a largely unchanged spatial pattern of correlations, with positive correlations located over the north coast of Papua New Guinea. Thus while the model broadly simulates the SST and precipitation anomalies associated with ENSO, regional biases over the coral site prevent direct comparison of precipitation variability at this location. Nevertheless, the lack of major changes in the simulated large-scale precipitation teleconnection patterns from the mid-Holocene to pre-industrial supports the interpretation of the coral records as showing a reduction in ENSO amplitude rather than a change in ENSO precipitation teleconnections.

5 Conclusions

The coral oxygen isotope records imply up to 60% reduction in ENSO amplitude in the mid-Holocene, while the model simulates a reduction of around 10%. Although the model and coral records are in qualitative agreement, the coral records provide evidence for a substantially larger reduction in ENSO amplitude than is simulated by the model. The difference between the model and proxy records could be due to changes in the local ENSO precipitation response at the coral site, as discussed above. The western Pacific ENSO precipitation teleconnection is unchanged in the simulated mid-Holocene climate, although this result may not be robust as the model is unable to reproduce the observed modern teleconnection at this location. Nonetheless, the majority

of palaeoclimate records of mid-Holocene ENSO, including the coral oxygen isotope records of Tudhope et al. (2001), indicate a more significant reduction in ENSO amplitude than is simulated by the model.

Alternatively, the model may not correctly capture the physical response of ENSO to the increased seasonality in the mid-Holocene. For example, the biases in the mean state of the model may reduce the convective response in the western Pacific to increased summer insolation and the resulting strengthening of trade winds in the late summer and autumn period which has been identified as a possible mechanism for damping El Niño events in mid-Holocene climate. Previous studies have also identified uncertainties in the model ENSO response to climate forcing which may depend on details of the model physics and resolution (Collins, 2000b). The uncertainties in model simulations of ENSO in past, present and future climate will be examined in a future study using versions of HadCM3 with perturbed physical parameters in the atmospheric model following the approach of the Quantifying Uncertainty in Model Predictions (QUMP) project (Murphy et al., 2004).

Acknowledgements. Paul Valdes provided assistance with the set-up for the mid-Holocene simulations. This work was funded by NERC as part of the RAPID programme.

Edited by: P. Fabian and J. L. Santos
Reviewed by: Paul Aharon and another referee

References

Bush, A. B. G.: Assessing the impact of Mid-Holocene insolation on the atmosphere-ocean system, Geophys. Res. Lett., 26, 99–102, 1999.

Clement, A. C., Seager, R., and Cane, M. A.: Suppression of El Niño during the mid-Holocene by changes in the Earth's orbit, Paleoceanography, 15, 731–737, 2000.

Clement, A. C., Cane, M. A. and Seager, R.: An orbitally driven tropical source for abrupt climate change, J. Clim., 14, 2369–2375, 2001.

Collins, M.: The El Niño-Southern Oscillation in the second Hadley Centre coupled model and its response to greenhouse warming, J. Clim, 13, 1299–1312, 2000a.

Collins, M.: Understanding uncertainties in the response of ENSO to greenhouse warming, Geophys. Res. Lett, 27, 3509–3512, 2000b.

Dai, A. and Wigley, T.: Global patterns of ENSO-induced precipitation, Geophys. Res. Lett., 27, 1283–1286, 2000.

Gagan, M. K., Ayliffe, L. K., Hopley, D., Cali, J. A., Mortimer, G. E., Chappell, J., McCulloch, M. T., and Head, M. J.: Temperature and surface-ocean water balance of the mid-Holocene tropical western Pacific, Science, 279, 1014–1018, 1998.

Gagan, M. K., Hendy, E. J., Haberle, S. G., and Hantoro, W. S.: Post-glacial evolution of the Indo-Pacific Warm Pool and El Niño-Southern Oscillation, Quaternary International, 118–199, 127–143, 2004.

Gordon, C., Cooper, C., Senior, C. A., Banks, H., Gregory, J. M., Johns, T. C., Mitchell, J. F. B., and Wood, R. A.: The simulation of SST, sea ice extent and ocean heat transports in a version of the Hadley Centre coupled model without flux adjustments, Clim. Dyn., 16, 147–168, 2000.

Inness, P. M., Slingo, J. M., Guilyardi, E., and Cole, J.: Simulation of the Madden-Julian Oscillation in a coupled general circulation model. Part II: The role of the basic state, J. Clim., 16, 365–382, 2003.

Koutavas, A., Lynch-Stieglitz, J., Marchitto, T. M., and Sachs, J. P.: El Niño-like pattern in Ice Age tropical Pacific sea surface temperature, Science, 297, 226–230, 2002.

Liu, Z., Brady, E. C., and Lynch-Stieglitz, J.: Global ocean response to orbital forcing in the Holocene, Paleoceanography, 18, 1041, doi:10.1029/2002PA000819, 2003.

Murphy, J. M., Sexton, D. M. H., Barnett, D. N., Jones, G. S., Webb, M. J., Collins, M., and Stainforth, D. A.: Quantification of modelling uncertainties in a large ensemble of climate change simulations, Nature, 430, 768–772, 2004.

Otto-Bliesner, B. L.: El Niño/La Niña and Sahel precipitation during the middle Holocene, Geophys. Res. Lett., 26, 87–90, 1999.

Otto-Bliesner, B. L., Brady, E. C., Shin, S.-I., Liu, Z., and Shields, C.: Modeling El Niño and its tropical teleconnections during the last glacial-interglacial cycle, Geophys. Res. Lett., 30, 2198, doi:10.1029/2003GL018553, 2003.

Pope, V. D., Gallani, M. L., Rowntree, P. R., and Stratton, R. A.: The impact of new physical parametrizations in the Hadley Centre climate model: HadAM3, Clim. Dyn., 16, 123–146, 2000.

Rayner, N. A., Parker, D. E., Horton, E. B., Folland, C. K., Alexander, L. V., Rowell, D. P., Kent, E. C., and Kaplan, A.: Global analyses of sea surface temperature, sea ice and night time marine air temperature since the late nineteenth century, J. Geophys. Res., 108, 4407, doi:10.1029/2002JD002670, 2003.

Rodbell, D. T., Seltzer, G. O., Anderson, D. M., Abbott, M. B., Enfield, D. B., and Newman, J. H.: An ∼15 000-year record of El Niño-driven alluviation in southwestern Ecuador, Science, 283, 516–520, 1999.

Sandweiss, D. H., Richardson, J. B., Reitz, E. J., Rollins, H. B., and Maasch, K. A.: Geoarchaeological evidence from Peru for a 5000 year B.P. onset of El Niño, Science, 273, 1531–1533, 1996.

Tudhope, A. W., Shimmield, G. B., Chilcott, C. P., Jebb, M., Fallick, A. E., and Dalgleish, A. N.:, Recent changes in climate in the far western equatorial Pacific and their relationship to the Southern Oscillation; oxygen isotope records from massive corals, Papua New Guinea, Earth Plan. Sci. Lett., 136–34, 575–590, 1995.

Tudhope, A. W., Chilcott, C. P., McCulloch, M. T., Cook, E. R., Chappell, J., Ellam, R. M., Lea, D. W., Lough, J. M., and Shimmield, G. B.: Variability in the El Niño-Southern Oscillation through a glacial-interglacial cycle, Science, 291, 1511–1517, 2001.

Turner, A. G., Inness, P. M., and Slingo, J. M.: The role of the basic state in the ENSO-monsoon relationship and implications for predictability, Q. J. R. Meteor. Soc., 131, 781–804, 2005.